# Synthetic dimensions in the strong-coupling limit: Supersolids and pair superfluids

Thomas Bilitewski* and Nigel R. Cooper
*T.C.M. Group, Cavendish Laboratory, J.J. Thomson Avenue, Cambridge CB3 0HE, United Kingdom*
(Received 29 June 2016; published 25 August 2016)

We study the many-body phases of bosonic atoms with $N$ internal states confined to a one-dimensional (1D) optical lattice under the influence of a synthetic magnetic field and strong repulsive interactions. The $N$ internal states of the atoms are coupled via Raman transitions creating the synthetic magnetic field in the space of internal spin states corresponding to recent experimental realizations. We focus on the case of strong SU($N$) invariant local density-density interactions in which each site of the 1D lattice is at most singly occupied, and strong Raman coupling, in distinction to previous work which has focused on the weak Raman coupling case. This allows us to keep only a single state per site and derive a low-energy effective spin-1/2 model. The effective model contains first-order nearest-neighbor tunneling terms, second-order nearest-neighbor interactions, and correlated next-nearest-neighbor tunneling terms. By adjusting the flux $\phi$, one can tune the relative importance of first-order and second-order terms in the effective Hamiltonian. In particular, first-order terms can be set to zero, realizing a model with dominant second-order terms. We show that the resulting competition between density-dependent tunneling and repulsive density-density interaction leads to an interesting phase diagram including a phase with long-range pair-superfluid correlations. The method can be straightforwardly extended to higher dimensions and lattices of arbitrary geometry, including geometrically frustrated lattices where the interplay of frustration, interactions, and kinetic terms is expected to lead to even richer physics.

DOI: 10.1103/PhysRevA.94.023630

## I. INTRODUCTION

Cold-atom systems provide an ideal setting in which to perform experiments that simulate quantum many-body systems. The fine control and wide tunability of system parameters, as well as precise measurements of observables, allow cold-atom systems to simulate idealized models of solid-state physics [1,2], making them a testing ground for condensed-matter theories. However, the natural situations that emerge in cold-atom experiments also introduce new models with interesting and novel features which raise new theoretical questions.

Optical lattices can be used to confine atoms in $d = 1,2,3$-dimensional lattices of chosen geometry. An additional synthetic dimension can be created in any $d$-dimensional lattice by exploiting the internal states, e.g., spin states, of the atoms [3,4]. Recent progress in the control of cold-atomic gases allows the study of systems with large (tunable) numbers of internal spin states [5–7]. Engineering the transitions between the internal states, e.g., by Raman transitions induced by lasers, allows the simulation of motion as along an additional (finite) "synthetic" dimension. Moreover, this synthetic dimension can also be used to engineer artificial gauge fields for neutral atoms [4,8,9], thus opening the possibility to explore topological physics in higher-dimensional settings. Experimentally, this has been realized in a one-dimensional (1D) lattice geometry realizing the physics and associated topological properties of a two-dimensional system [10,11]. More recently, it has been proposed how one could simulate four-dimensional quantum Hall physics in cold-atom setups using these techniques [12].

In this work, we will focus on one-dimensional systems with a finite synthetic dimension composed of $N = (2I + 1)$ spin states coupled by laser beams in such a way as to create an artificial magnetic field. Thus, they can alternatively be considered as frustrated $N$-leg ladders. Optical lattice experiments with cold atoms motivate the study of both bosonic [13–18] and fermionic [19–28] systems. The predicted behavior includes chirally ordered phases [14], vortex phases [16], magnetic crystals, and quasi-1D analogues of fractional quantum Hall states [25,27,28]. At the center of these phenomena is the interplay of the gauge fields and the SU($2I + 1$) symmetric interactions [29–32]. The natural SU($2I + 1$) symmetry of the interactions between the spin states implies, in the interpretation of a ladder, that the interactions are infinitely ranged along the synthetic dimension and short-ranged along the real dimension, in contrast to the situation usually considered in the solid-state context. We remark that therefore the limit of hardcore interactions of bosonic particles does not correspond to a Tonks-Girardeau gas [33–35] and the system does not reduce to free fermions.

Prior studies have focused on the weak Raman coupling case in which one obtains helical states and edge currents [28]. In contrast, we will study the case of strong Raman coupling and strong interactions, focusing on an effective model of hard-core bosons in these limits which can alternatively be understood in terms of an effective pseudo-spin-1/2 system. Our main focus will be on a regime in which the physics is dominated by the interplay of density-density interactions and correlated tunneling terms. This will lead to a competition between phase separation and charge order, and normal superfluidity and pair superfluidity.

In 2D, pair superfluids can be realized using the long-range interactions of dipolar quantum gases [36,37] and confining them in bilayer geometries [38–40]. In a mean-field analysis, the presence of correlated tunneling allows the condensation of pairs ($\langle b_i b_j \rangle \neq 0$) in the absence of single-particle condensation ($\langle b_i \rangle = 0$) [41]. Generically, correlated tunneling can be understood to act as an attractive

*tb494@cam.ac.uk

 

interaction between the bosons favoring pair formation, and the repulsive nearest-neighbor interaction is required to avoid collapse [42] or phase separation [43]. Correlated tunneling has been shown to lead to pair superfluidity for bosons in 2D [43] and in 1D [44,45] in theoretical studies, but the required models are hard to realize experimentally.

We propose a way to realize (quasi)-pair-condensed and supersolid phases of ultracold atoms starting from an experimentally realized system. We do not require special (long-range) interactions or complicated lattice geometries. The proposed scheme is applicable to both fermions and bosons, but we will limit the discussion to the bosonic case here. We do not assume specially engineered Raman couplings of the spin states to obtain homogeneous couplings along the synthetic dimension or periodic boundary conditions, which are hard to realize experimentally for large number of internal spin states, but consider the highly nonhomogeneous couplings and open boundary conditions along the synthetic dimension, which occur naturally for $I > 1$ due to the nature of the atom-light interaction.

We introduce the full model and the effective model derived in the limits of large Raman coupling and strong interactions in Sec. II. Importantly, the coupling constants will turn out to depend on the flux $\phi$, and the freedom in tuning both the flux and the number of spin states $2I + 1$ allows great control and freedom in engineering the resulting effective Hamiltonian. In Sec. III, we will focus on the special case of flux $\phi = \pi$ in which the first-order terms vanish and investigate the behavior resulting from the dominant second-order terms in the effective model. By employing density matrix renormalization group (DMRG) calculations [46], the phase diagram of the effective model is obtained, and described in Sec. III. Based on the analysis of correlation functions and the von Neumann entropy, we establish a phase diagram containing a charge density wave (CDW) at half filling, a supersolid (SS) phase with simultaneous charge density wave order and superfluid correlations, and a (quasi)-pair-superfluid phase.

## II. MODEL

We consider spinful bosons with $N = 2I + 1$ internal spin states loaded into a one-dimensional optical lattice described by a Hamiltonian $\hat{H} = \hat{H}_1 + \hat{H}_2 + \hat{H}_{\text{int}}$. $\hat{H}_1$ describes the bosonic hopping along the lattice, $\hat{H}_1 = -t \sum_j \sum_{m=-I}^{I} (\hat{c}^\dagger_{j+1,m} \hat{c}_{j,m} + \text{H.c.})$ where $\hat{c}^{(\dagger)}_{j,m}$ are bosonic operators annihilating (creating) bosons in spin state $m$ at site $j$, and $t$ is the hopping amplitude. $\hat{H}_2$ describes the Raman coupling of the internal spin states via $\hat{H}_2 = -\sum_j \sum_{m=-I}^{I-1} \Omega_{m+1} (e^{i\phi j} \hat{c}^\dagger_{j,m+1} \hat{c}_{j,m} + \text{H.c.})$ where $\Omega_m = \Omega g_m$ with $g_m = \sqrt{I(I+1) - m(m-1)}$, and $\phi$ is the running phase of the Raman beams (set by the wave-vector transfer $\Delta k$ and the lattice constant $d$). $\hat{H}_{\text{int}}$ is taken to be an SU$(2I + 1)$ invariant interaction of contact form, i.e., $\hat{H}_{\text{int}} = U \sum_{j,m,m'} \hat{n}_{j,m} (\hat{n}_{j,m'} - \delta_{m,m'})$. In the next section, we will consider an effective spin-1/2 model describing the dynamics in the strong-coupling limit.

### Effective model at strong coupling

We will consider the parameter regime $t \ll \Omega, U$ and work with the resulting low-energy effective Hamiltonian in the following. In the limit $t \ll \Omega$, only the lowest of the eigenstates of $\hat{H}_2$ remains in the effective description coupled via direct and virtual hoppings induced by $\hat{H}_1$. The interaction $\hat{H}_{\text{int}}$ takes the same form in the eigenbasis of $\hat{H}_2$ due to its SU$(2I + 1)$ invariance and, in the limit of $t \ll U$, leads to a hard-core constraint in the effective basis. In the Appendix, A we derive the effective second-order model describing spinless particles interacting via a nearest-neighbor interaction and hopping with nearest-neighbor, next-nearest-neighbor, and correlated next-nearest-neighbor tunneling terms.

The effective Hamiltonian takes the form

$$\begin{aligned} \hat{H}_{\text{eff}}/t = &-t_1(\phi) \sum_j (\hat{d}^\dagger_{j+1} \hat{d}_j + \text{H.c.}) + \kappa V(\phi, \tilde{u}) \sum_l \hat{n}_l \hat{n}_{l+1} \\ &-\kappa t_2(\phi, \tilde{u}) \sum_j (\hat{d}^\dagger_{j+2} \hat{d}_j + \text{H.c.}) \\ &+\kappa t_{\text{cor}}(\phi, \tilde{u}) \sum_j (\hat{d}^\dagger_{j+2} \hat{n}_{l+1} \hat{d}_j + \text{H.c.}), \end{aligned} \tag{1}$$

where $\hat{d}_j = \hat{d}_{j,I}$ is the creation operator for a particle in the $s_x = I$ (after the unitary transformation explained in the Appendix A) eigenstate at site $j$, $\kappa = t/\Omega$, and $\tilde{u} = U/(4\Omega I)$. The explicit form and functional dependence of the coupling constants on the flux $\phi$, the interaction strength $\tilde{u}$, and the number of spin states $I$ is provided in the Appendix A; see Eqs. (A5)–(A7).

The first term describes the direct hopping between the $s_x = I$ spin state on neighboring lattice sites, with an energy scale that is reduced from the bare hopping $t$ by the factor $t_1(\phi) = (\cos\phi/2)^{2I}$ [Eq. (A5)]. The remaining terms describe virtual hopping processes, with energy scale proportional to $t\kappa = t^2/\Omega$. The nearest-neighbor repulsion $V$ contains three contributions, originating from nearest-neighbor hopping and returning to the original site via an excited spin state on a neighboring site which is either empty, occupied, or hopping onto an occupied site in the lowest-energy spin state. The correlated tunneling term $t_{\text{cor}}$ arises from the corresponding processes with the particle not returning to the original site. These processes are illustrated in Fig. 1(a).

Importantly, the virtual hopping between the different Raman eigenstates is controlled by $\kappa = t/\Omega$. To avoid double occupancy, we only require $t_1(\phi) \ll U/t$, which can be achieved even if the bare coupling $t$ is large by making $t_1(\phi)$ small through a judicious choice of $\phi$. This allows us to work at relatively high-energy scales using shallow lattices with high bare tunneling rates $t$, in contrast to the induced interactions in the Mott regime of the Hubbard model scaling with $t/U$ requiring deeper lattices and lowering the overall energy scale. Further, the dependence of the coupling constants on the flux $\phi$ allows one to eliminate the first-order tunneling terms and obtain an effective model with dominant second-order terms, even for relatively shallow lattices where all energy scales remain large.

## III. MODEL AT $\phi = \pi$

In the following, we focus on the model at flux $\phi = \pi$. Then, the first-order nearest-neighbor tunneling term $t_1(\phi)$ vanishes identically and the effective model is determined by

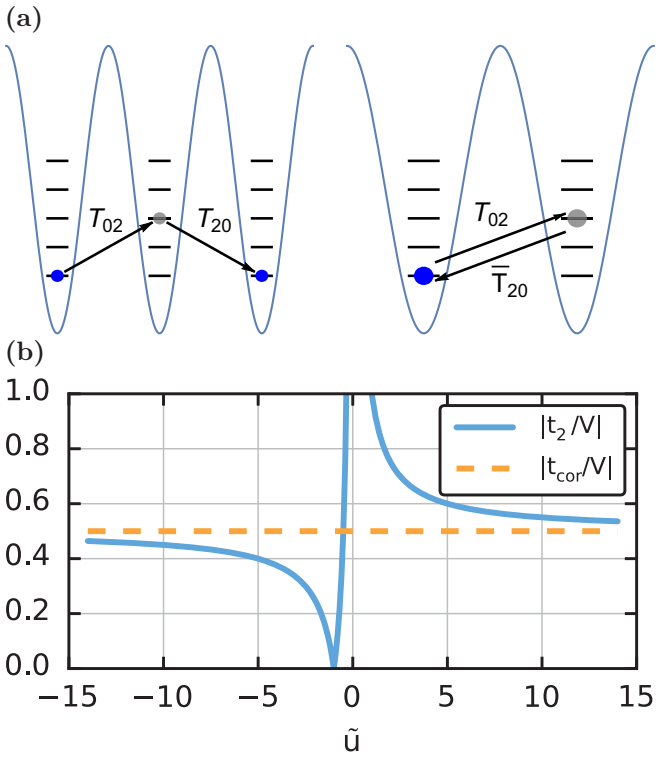


FIG. 1. (a) Second-order virtual processes in the effective Hamiltonian given by Eq. (1) illustrated in the case of $I = 2$. The left shows a particle hopping into an excited state on an unoccupied site and back to the ground state and leads to a normal and a correlated NN hopping term $t_2$ and $t_{\rm cor}$; hopping via an occupied site leads to $t_{\rm cor}$. The right corresponds to hopping back and forth via an excited state and leads to an effective NN interaction $V$ of particles on neighboring sites. (b) Coupling constants $t_2/V$ and $t_{\rm cor}/V$ as a function of rescaled interaction $\tilde{u} = U/(4\Omega I)$ of the effective spin-1/2 model at flux $\phi = \pi$; see Eq. (2).

the second-order terms only. The model reduces to

$$\hat{H}_{\rm eff}/(t\kappa) = V\sum_j \hat{n}_j\hat{n}_{j+1} - t_2\sum_j(\hat{c}_j^\dagger\hat{c}_{j+2} + \text{H.c.}) + V/2\sum_j(\hat{c}_j^\dagger\hat{n}_{j+1}\hat{c}_{j+2} + \text{H.c.}), \quad (2)$$

where $c_j^\dagger$ is the creation operator for hard-core bosons at site $j$, $n = c_j^\dagger c_j$ is the corresponding density, and the couplings are the ones defined below Eq. (1) for $\phi = \pi$. Note that in these limits, $t_{\rm cor} = V/2$. Since the nearest-neighbor (NN) tunneling term has dropped out, particles now only hop on their respective $A/B$ sublattices, and the model can therefore also be understood to live on a "zigzag" lattice.

To gain some understanding of the effective model, we first consider the more general case in which all coupling constants can be tuned independently, i.e., we consider the model with couplings $t_2, t_{\rm cor}$, and $V$. Note that those correspond to two-body, three-body, and four-body terms, respectively. For $t_{\rm cor} = V = 0$, the model is noninteracting and describes free hard-core bosons living separately on each sublattice. For $t_{\rm cor} = 0$, the model corresponds to the $t_2 - V$ model [47]. It has been shown to undergo a quantum phase transition from a superfluid (SF) phase to a supersolid (SS) phase at nonhalf filling and to a charge density wave (CDW) at exactly half filling as a function of $t_2/V$. For $V = 0$, the model is integrable and known as Bariev's model [48]; in this limit, we have two next-nearest-neighbor (NNN) hopping terms, i.e., a normal hopping $t_2$ and a correlated hopping $t_{\rm cor}$ for which hopping between sites depends on the occupation of the intermediate site on the other sublattice. Depending on $t_{\rm cor}/t_2$, the model has a finite CDW amplitude, i.e., different sublattice populations, in the ground state. The fermionic spin-1/2 version of this model has recently been studied in Ref. [49]. For $V = 0$ and $t_{\rm cor} = t_2$, the model admits an exact solution via a mapping to free spinless particles moving on a charge lattice. This solution becomes possible because for $t_{\rm cor} = t_2$ particles cannot pass each other, and the sequence of particles remains preserved throughout the dynamics. The ground state of the model is found to be a paired-hole superconductor with hidden string order and algebraically decaying two-particle correlations.

For our model, we are not free to choose these couplings independently. The dependence of the couplings in the effective model given by Eq. (2) on the rescaled interaction strength $\tilde{u} = U/(4\Omega I)$ is shown in Fig. 1(b). In these limits, we obtain $t_{\rm cor}/V = 0.5$ and $t_2/V = (1+\tilde{u})/(2\tilde{u})$. Thus, the model depends only on a single free parameter $\tilde{u}$, which determines the ratio $t_2/V$, or we can alternatively consider the model as a function of $t_2/V$. Hard-core interactions correspond to $t_2/V = 0.5$ and we will consider the region of repulsive interactions corresponding to $t_2/V \geqslant 0.5$ in Sec. III. We note that with these parameters, we are outside of the integrable limits described above and it will be interesting to see what remains of the physics in the parameter regime accessible in our model.

### Phase diagram

To characterize the ground-state phases, we perform DMRG simulations using the ALPS matrix-product state (MPS) framework [50,51]. We consider system sizes of $L = 80, 120, 160, 240$ with open boundary conditions keeping a maximal number of states of $m = 400, 600, 800$, extrapolating results for fixed system size in $1/m$. To characterize the ground state and obtain the phase diagram, we study two- and four-point correlation functions and the structure factors for CDW, superfluid, and pair-superfluid order. To reduce the effects of the open boundary conditions, correlators are measured from the middle of the system and averaged over a window of 10 sites around the central site. We perform finite-size scaling of the corresponding correlation lengths, decay exponents, and structure factors to obtain the phase boundaries. In addition, we characterize the phases via their entanglement entropy and central charge.

On a bipartite lattice, due to the vanishing of the nearest-neighbor tunneling, the sublattice populations $n_{A(B)} = \sum_{i\in A(B)} n_i$ are separately conserved, and we focus on equal populations on both sublattices $n_A = n_B$. The phase diagram of the model as a function of $t_2$ in the range $0.5 \leqslant t_2/V \leqslant 0.64$ and density $0 \leqslant n \leqslant 1$ is shown in Fig. 2. Three distinct phases are observed in this parameter range: a charge density wave (CDW) with a period of two lattice sites, a supersolid (SS) with simultaneous (quasi)superfluid and maximal CDW order,

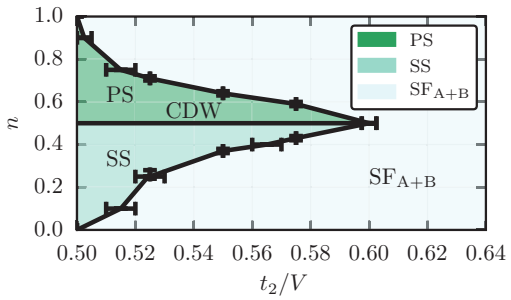


FIG. 2. Phase diagram of the effective model given by Eq. (2) obtained from the DMRG calculations as a function of coupling $t_2$ and density $n$. Three distinct phases are observed: a gapped CDW at $n = 0.5$ and $t_2 \leqslant 0.6$, a supersolid (SS) phase with superfluid order on one of the sublattices with the other sublattice being empty with central charge $c = 1$ below half filling $n < 0.5$, and a homogeneous phase with dominant superfluid (SF$_{A+B}$) order on both lattices with $c = 2$ for high densities $n$ and high $t_2$, which also shows strong pair-superfluid correlations. Above half filling at low $t_2$, we find phase separation (PS) as indicated in a jump in $n(\mu)$.

and a homogeneous phase with (quasi)superfluidity on both sublattices (SF$_{A+B}$) with pair-superfluid correlations. Since we consider the case of $n_A = n_B$, both the CDW and the SS phases are additionally separated into a left or right region with vanishing density on one of the sublattices in both regions. Before the transition into the SF$_{A+B}$ phase, the maximally imbalanced state with $N_A = N$, $N_B = 0$ (or the equivalent state with $N_A = 0$, $N_B = N$) is slightly lower in energy, and degenerate in the thermodynamic limit. Both the balanced and the maximally imbalanced state are realized as thermodynamic phases when introducing two chemical potentials $\mu_A$ and $\mu_B$ coupling to the respective densities. Our discussion of the properties of the state does not rely on this distinction. After the transition into the SF$_{A+B}$, the imbalanced state is energetically disfavored.

Exactly at half filling $n = 0.5$, the CDW phase is stabilized and persists up to $t_2/V = 0.6$. Below half filling $n < 0.5$ at low coupling $t_2$, the effects of the nearest-neighbor repulsion are still dominant, resulting in a phase where one of the sublattices is empty and the other is filled and becomes (quasi)superfluid, thus forming a supersolid state. We remark that if one sublattice is empty, the model reduces to free particles hopping on the other sublattice with amplitude $t_2$. Above half filling $n > 0.5$ at low $t_2$, particles cannot avoid the cost of the interaction energy $V$ and the system phase separates. At sufficiently high $t_2$, the effect of the repulsion $V$ can be overcome and a homogeneous phase with superfluid order on both lattices emerges. In this regime, all of $t_2$, $t_{\rm cor}$, and $V$ are relevant.

An important tool to characterize the ground-state behavior of strongly correlated systems in one dimension is the von Neumann block entropy [52]. This is defined as $S_A^N = \mathrm{Tr}\,\rho_A \ln \rho_A$, where $\rho_A$ is the reduced density matrix $\rho_A = \mathrm{Tr}_B \rho$ obtained by dividing the chain into the block $A$ consisting of sites $i = 1, \ldots, l$ and $B$ of sites $i = l+1, \ldots, L$. In particular, for a gapped state, the entropy saturates whereas it diverges for a gapless state [53,54]. For a 1D system of size $L$ with open boundary conditions, the von Neumann block entropy behaves as $S_L^N(l) = s_1 + \frac{c}{6} \ln[\frac{2L}{\pi} \sin(\frac{\pi l}{L})]$, where $c$ is the central charge

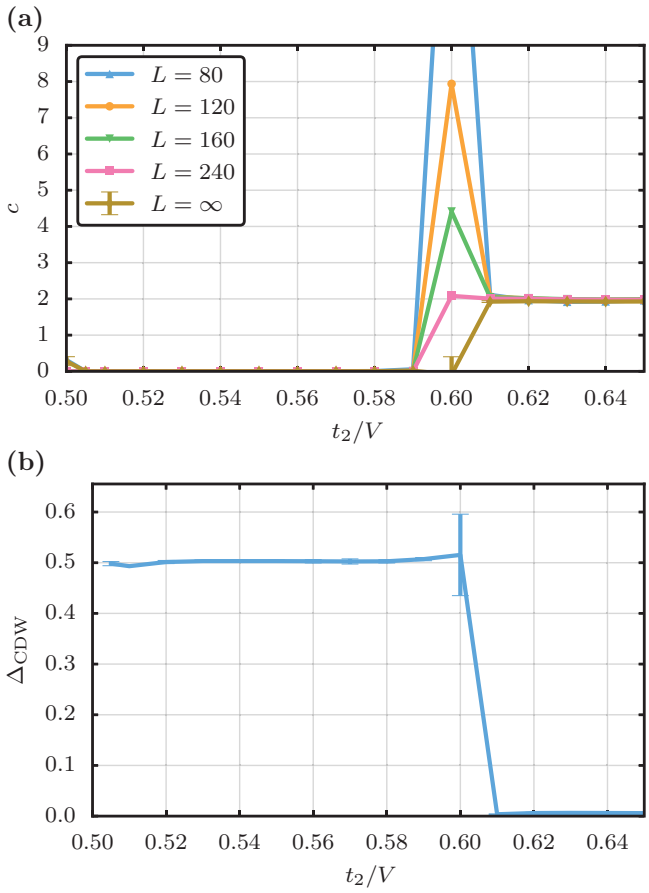


FIG. 3. (a) The central charge $c$ determined from fitting the von Neumann block entropy via $S_L^N(l) = \frac{c}{6} \ln[\frac{2L}{\pi} \sin(\frac{\pi l}{L})]$ for different system sizes as a function of the coupling $t_2$ at density $n = 0.5$. The CDW is gapped and the transition occurs into the SF$_{A+B}$ phase with central charge $c = 2$. (b) Extrapolated CDW order parameter $\Delta_{\rm CDW} = \lim_{L\to\infty} \sqrt{|1/L \sum_l e^{i\pi l} G(l)|}$ at density $n = 0.5$ as a function of coupling $t_2$ showing the vanishing of CDW order at $t_2/V = 0.61$.

of the associated conformal field theory (CFT) and $s_1$ is a nonuniversal constant [55–57]. By fitting $S_L^N$ linearly in the conformal distance $\lambda = \ln[\frac{2L}{\pi} \sin(\frac{\pi l}{L})]$, we obtain the central charge $c$ of the phase. The behavior of the central charge $c$ as a function of the coupling $t_2$ at density $n = 0.5$ is shown in Fig. 3(a). The results indicate a transition close to $t_2/V = 0.6$. The state for $t_2/V \leqslant 0.6$ is gapped as expected for the CDW phase and the transition occurs into a state with central charge of $c = 2$ in the SF$_{A+B}$. Finally, below half filling, we find a central charge $c = 1$ (not shown), which is consistent with superfluidity on one of the sublattices in the SS phase.

The CDW order can be directly extracted from the density-density correlation and the static structure factor. We measure $G(l) = \langle \hat{n}_i \hat{n}_{i+l} \rangle$. The static structure factor is defined as $S_L(q) = 1/L \sum_l e^{iql} G(l)$. The CDW order parameter is given by the square root of the structure factor at $q = \pi$, $\Delta_{\rm CDW}(L) = \sqrt{|S_L(\pi)|}$, and its infinite system size limit, $\Delta_{\rm CDW} = \lim_{L\to\infty} \sqrt{|S_L(\pi)|}$. The finite system results $\Delta_{\rm CDW}(L)$ are extrapolated via a quadratic fit in $1/L$ to infinite system size. The results of this extrapolation are shown in

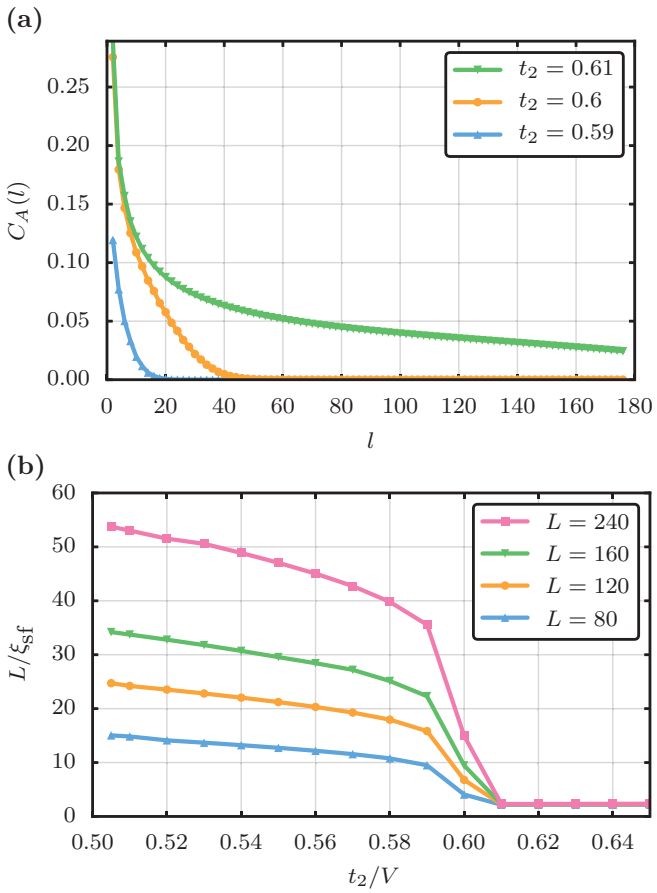


FIG. 4. (a) Two-point correlation function $C_\alpha(l)$ as a function of $l$ on sublattice $A$ ($\alpha = 0$) for a system of size $L = 240$ at density $n = 0.5$ for $t_2/V = 0.61, 0.6, 0.59$ (top to bottom) showing the transition from short-range to long-range correlations at $t_2/V = 0.61$. (b) System size $L$ divided by superfluid correlation length $\xi_{sf}$ for sublattice $A$ vs coupling $t_2$ for $L = 240, 160, 120, 80$ (top to bottom). Coalescence of data points for different $L$ at $t_2/V = 0.61 \pm 0.05$ signals transition to SF state.

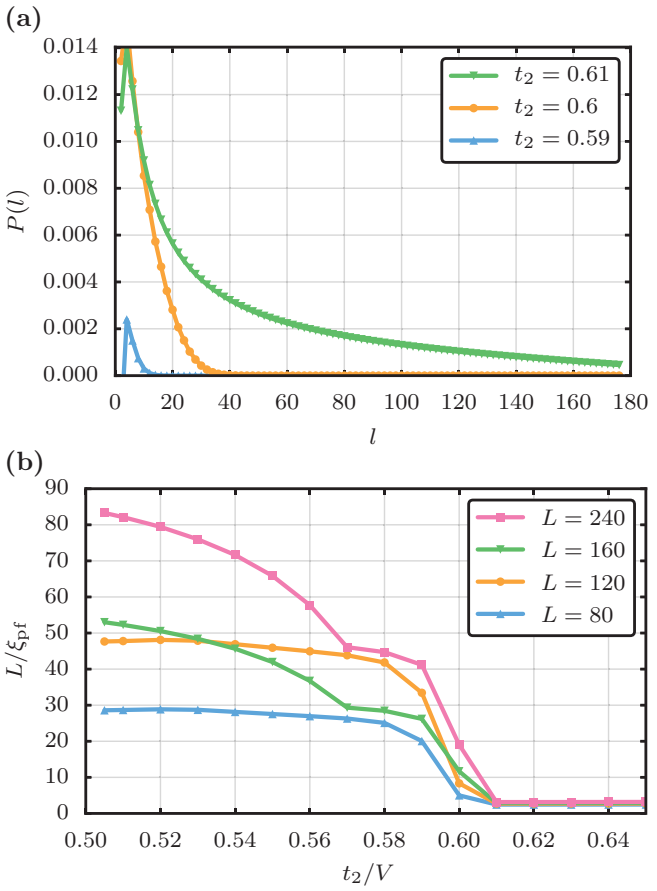


FIG. 5. (a) Four-point correlation function $P(l)$ as a function of $l$ for a system of size $L = 240$ at density $n = 0.5$ for $t_2/V = 0.61, 0.6, 0.59$ (top to bottom) showing the transition from short-range to long-range correlations at $t_2/V = 0.61$. (b) System size $L$ divided by pair-superfluid correlation length $\xi_{pf}$ vs coupling $t_2$ for $L = 240, 160, 120, 80$ (top to bottom). Coalescence of data points for different $L$ at $t_2/V = 0.61 \pm 0.05$ signals transition to pair superfluid (PSF) state.

Fig. 3(b). The CDW order parameter vanishes at $t_2/V = 0.61$, signaling the transition into the superfluid state.

To characterize the degree of (quasi)superfluid order, we consider the two-point correlation function $C_\alpha(2l) = \langle \hat{c}^\dagger_{2i+\alpha} \hat{c}_{2i+\alpha+2l} \rangle$ on either sublattice ($\alpha = 0, 1$). This correlation function is shown in Fig. 4(a) for a system of size $L = 240$ on sublattice $A$ ($\alpha = 0$) displaying a transition from short-range to long-range correlations around $t_2/V = 0.61$; the other sublattice (not shown) exhibits the same behavior. In contrast to CDW, there is no order parameter for superfluidity in one dimension, and the whole superfluid phase is critical. Still, the superfluid phase is characterized by a diverging correlation length [58]. To determine the transition point, we perform finite-size scaling of the correlation length defined as $\xi_{sf} = \sqrt{\sum_l l^2 C_\alpha(l) / \sum_l C_\alpha(l)}$ [59,60]. In Fig. 4(b), $L/\xi_{sf}$ on sublattice $A$ ($\alpha = 0$) is shown as a function of $t_2$ at $n = 0.5$ for different system sizes; the correlations on sublattice $B$ show the same behavior. The coalescence of the data signals the transition to the superfluid state at $t_2/V = 0.61$. In the superfluid phase, we find strong correlations between the superfluids on the sublattices. To characterize this phase further, we also consider possible condensation of pairs via $P(2l) = \langle \hat{c}^\dagger_{2i} \hat{c}^\dagger_{2i+1} \hat{c}_{2i+2l} \hat{c}_{2i+1+2l} \rangle - \langle \hat{c}^\dagger_{2i} \hat{c}_{2i+2l} \rangle \langle \hat{c}^\dagger_{2i+1} \hat{c}_{2i+1+2l} \rangle$ and its corresponding correlation length $\xi_{pf} = \sqrt{\sum_l l^2 P(l) / \sum_l P(l)}$. The pair-superfluid correlator is shown in Fig. 5(a) and the finite-size scaling of the correlation length in Fig. 5(b). We observe very strong pair-superfluid correlations in the $SF_{A+B}$ phase consistent with quasicondensation of pairs as the system becomes superfluid. However, single-particle superfluidity persists alongside pair superfluidity in the parameter regime we have studied.

In Figs. 6(a) and 6(b), we display the momentum distribution of particles on sublattice $A$, $n(q) = \sum e^{iql} C_A(l)$, and in Figs. 6(c) and 6(d), the momentum distribution of pairs of particles $n_{pf}(q) = \sum e^{iql} P(l)$. As for hard-core bosons, $n(q = 0)$ is expected to scale with $\sqrt{L}$ [61], and both quantities are normalized by this factor. We focus on the transition from the SS phase in Figs. 6(a) and 6(c) to the $SF_{A+B}$ phase in Figs. 6(b) and 6(d). Whereas in the single-particle momentum distribution a quasicoherent peak is observed in both phases,

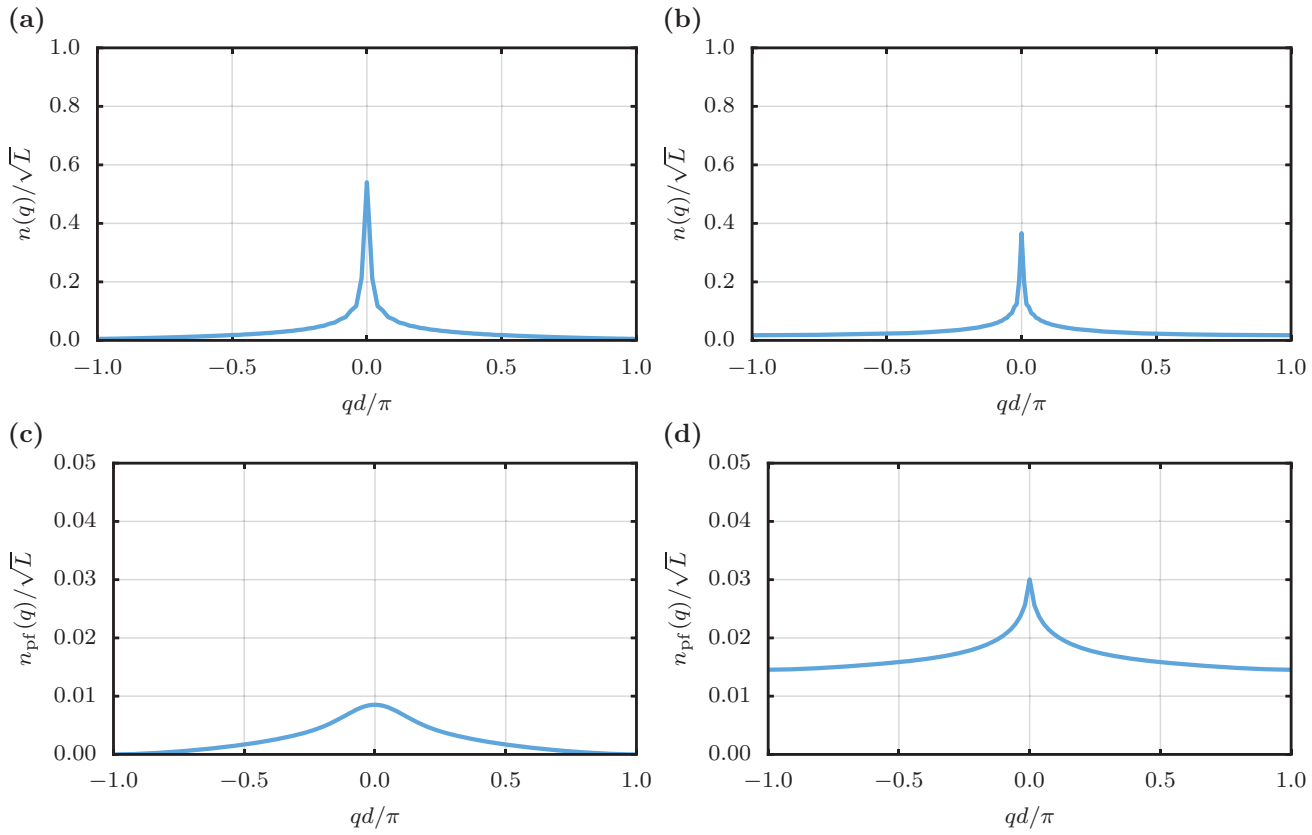


FIG. 6. (a),(b) Single-particle momentum distribution $n(q) = \sum e^{iql} C_A(l)$ on sublattice $A$. (c),(d) Momentum distribution for pairs of particles $n_{\mathrm{pf}}(q) = \sum e^{iql} P(l)$. All are at density $n = 0.25$ and (a) and (c) at $t_2/V = 0.51$ in the SS phase and (b) and (d) at $t_2/V = 0.55$ in the $\mathrm{SF}_{A+B}$ phase. The single-particle momentum distribution shows a quasicoherent peak in both phases (a) and (b). In contrast, for pairs in the SS phase in (c), no quasicoherent peak is observed, whereas a peak forms in the $\mathrm{SF}_{A+B}$ phase in (d).

pairs only quasicondense in the $\mathrm{SF}_{A+B}$ phase as seen in Fig. 6(d).

## IV. CONCLUSIONS

In summary, in this work we have shown that the interplay of (synthetic) gauge fields and interactions in ultracold gas systems leads naturally to effective Hamiltonians with correlated hopping terms. We start from an experimentally feasible setup for the creation of an artificial magnetic field using synthetic dimensions. We consider this model in the limits of strong Raman coupling of the spin states and strong interactions where it reduces to an effective model with first-order nearest-neighbor tunneling, second-order next-nearest-neighbor correlated tunneling terms, and nearest-neighbor repulsion. Importantly, the additional degree of freedom given by adjusting the flux $\phi$ allows one to engineer effective models dominated by second-order processes with large energy scales.

By working at flux $\phi = \pi$, the first-order nearest-neighbor tunneling term is eliminated, and we obtain a model with dominant second-order terms. This is a natural route to a large density-dependent tunneling term, so the proposed scheme is directly relevant to the realization and study of models with interaction-assisted hopping and kinetic frustration [62–68].

The physics of our effective model involves the competition between the correlated tunneling, which favors pair formation, and the nearest-neighbor repulsion, which favors local CDW order. We find three distinct phases: a CDW phase, a supersolid (SS) phase with simultaneous quasisuperfluidity on either sublattice and maximal CDW order, and a quasisuperfluid on both sublattices with strong pair-superfluid correlations $\mathrm{SF}_{A+B}$.

The model can be directly generalized to fermionic species and higher-dimensional lattices of arbitrary geometry. In the case of fermions, the study of attractive interactions seems particularly relevant for the study of paired phases. The extension to higher dimensions promises even more interesting physics, e.g., Berezinskii-Kosterlitz-Thouless (BKT) transitions to novel superconducting states and geometrically frustrated magnetism. We reserve the discussion of the resulting phases for future work.

## ACKNOWLEDGMENTS

The DMRG calculations have been performed using the ALPS libraries [50,51]. T.B. would like to thank A. Läuchli for helpful discussions and comments. T.B. acknowledges insightful correspondence with H. Katsura who pointed out the relation of our effective model to the integrable Bariev-model in 1D. This work was supported by EPSRC Grant No. EP/K030094/1. Statement of compliance with EPSRC

policy framework on research data: All data accompanying this publication are directly available within the publication.

## APPENDIX: DERIVATION OF EFFECTIVE MODEL

We start from the Hamiltonian of bosons with $N = 2I + 1$ internal spin states loaded into a one-dimensional optical lattice described by $\hat{H} = \hat{H}_1 + \hat{H}_2 + \hat{H}_{\rm int}$.

$\hat{H}_1$ describes the bosonic hopping along the lattice,

$$\hat{H}_1 = -t \sum_j \sum_{m=-I}^{I} (\hat{c}^\dagger_{j+1,m} \hat{c}_{j,m} + \text{H.c.}), \tag{A1}$$

where $\hat{c}^{(\dagger)}_{j,m}$ are bosonic operators annihilating (creating) bosons in spin state $m$ at site $j$, and $t$ is the hopping amplitude.

In addition, the internal spin states are coupled by Raman lasers described by the Hamiltonian

$$\hat{H}_2 = -\sum_j \sum_{m=-I}^{I-1} \Omega_{m+1} (e^{i\phi j} \hat{c}^\dagger_{j,m+1} \hat{c}_{j,m} + \text{H.c.}), \tag{A2}$$

where $\Omega_m = \Omega g_m$ with $g_m = \sqrt{I(I+1) - m(m-1)}$, and $\phi = \Delta k_R d$ is the running phase of the Raman beams given by the wave-vector transfer $\Delta k_R$ and the lattice spacing $d$. $\hat{H}_{\rm int}$ is taken to be a SU$(2I + 1)$ invariant interaction of contact form, i.e., $\hat{H}_{\rm int} = U \sum_{j,m,m'} \hat{n}_{j,m} (\hat{n}_{j,m'} - \delta_{m,m'})$.

For open boundary conditions in the synthetic direction using the unitary transformation $\hat{U}$ defined by $\hat{U} \hat{c}_{j,m} \hat{U}^\dagger = e^{i\phi m j} \hat{c}_{j,m}$, the Hamiltonian is transformed to

$$\begin{aligned} \hat{U} \hat{H} \hat{U}^\dagger = &-t \sum_j \sum_{m=-I}^{I-1} (e^{-i\phi m} \hat{c}^\dagger_{j+1,m} \hat{c}_{j,m} + \text{H.c.}) \\ &- \sum_j \sum_{m=-I}^{I-1} \Omega_m (\hat{c}^\dagger_{j,m+1} \hat{c}_{j,m} + \text{H.c.}) + \hat{H}_{\rm int}. \end{aligned} \tag{A3}$$

As we consider $t \ll \Omega$, we now transform to the eigenstates of the Raman coupling Hamiltonian $\hat{H}_2$. After the unitary transformation, this is just $\hat{H}_2 = -2\Omega \sum_j \hat{\mathcal{S}}_{x,j}$, where $\hat{\mathcal{S}}_{x,j}$ is the $\hat{\mathcal{S}}_x$ operator for spin $I$ for particles at site $j$. Note in particular that it is now site independent due to gauging the Raman phase into the hopping part of the Hamiltonian. Consequently, the eigenfunctions are just the $s_x$ eigenstates and the spectrum at each site is given by $E_s = -2\Omega s$, with $s = -I, \ldots, I$. Due to the gauge transformation that we performed, this actually corresponds to a rotating spin orientation in the original basis.

$\hat{H}_1$ in the new basis reads as $\hat{H}_1 = -t \sum_{s,s'} [T_{s,s'}(\phi) \hat{d}^\dagger_{j+1,s'} \hat{d}_{j,s} + \text{H.c.}]$, where $\hat{d}^\dagger_{j+1,s'}$ creates a particle in the $s'_x$ eigenstate at site $j$ and we defined the hopping matrix $T_{s,s'}(\phi) = \langle s_x | e^{-i\phi \hat{\mathcal{S}}_z} | s'_x \rangle$ which now couples states $s$ and $s'$. As the interaction Hamiltonian is SU$(2I + 1)$ invariant, it takes the same form in the transformed basis, $\hat{H}_{\rm int} = U \sum_{j,s,s'} \hat{n}_{j,s} (\hat{n}_{j,s'} - \delta_{s,s'})$, where now the sum runs over the $s_x$ eigenstates. In the limit of strong interactions, this restricts the occupation at each site to be 0 or 1.

We see that $\hat{H}_2 + \hat{H}_{\rm int}$ is diagonal in the occupation number basis of $s_x$ eigenstates. In the limit $t \ll \Omega, U$, we treat $\hat{H}_1$ as a perturbation and derive an effective model keeping only the lowest-energy eigenstate at each site, i.e., the $s = I$ state, and consider the sector with empty and singly occupied sites. To second order, we obtain a model describing spinless particles interacting via a nearest-neighbor interaction and hopping with nearest-neighbor, next-nearest-neighbor, and correlated next-nearest-neighbor tunneling terms. The effective Hamiltonian takes the form

$$\begin{aligned} \hat{H}_{\rm eff}/t = &-f^I_t(\phi) \sum_j (\hat{d}^\dagger_{j+1} \hat{d}_j + \text{H.c.}) \\ &+ 2\kappa \left[ f^I_V(\phi, \tilde{u} = 0) - f^I_V(\phi, \tilde{u}) - \frac{f^I_t(\phi)^2}{2I\tilde{u}} \right] \sum_l \hat{n}_l \hat{n}_{l+1} \\ &+ \kappa \Bigg\{ f^I_{\rm cor}(\phi, \tilde{u} = 0) \sum_j [\hat{d}^\dagger_{j+2} (1 - \hat{n}_{l+1}) \hat{d}_j + \text{H.c.}] \\ &+ f^I_{\rm cor}(\phi, \tilde{u}) \sum_j (\hat{d}^\dagger_{j+2} \hat{n}_{l+1} \hat{d}_j + \text{H.c.}) \\ &- \frac{f^I_t(\phi)^2}{2I\tilde{u}} \sum_j (\hat{d}^\dagger_{j+2} \hat{n}_{l+1} \hat{d}_j + \text{H.c.}) \Bigg\}, \end{aligned} \tag{A4}$$

where $\hat{d}_j = \hat{d}_{j,I}$ is the creation operator for a particle in the $s_x = I$ eigenstate at site $j$, $\kappa = t/\Omega$, and $\tilde{u} = U/(4I\Omega)$.

The functions $f^{(I)}_i(\phi)$ depend on the flux $\phi$, the interaction strength $\tilde{u}$, and parametrically on the number of spin states $I$. The first term describes the diagonal hopping between the $s = I$ spin states and the remaining terms describe virtual hopping processes. The nearest-neighbor repulsion $V$ originates from nearest-neighbor hopping and returning to the original site via an excited spin state on a neighboring site which is either empty (first term), occupied (second term), or hopping onto an occupied site in the lowest-energy spin state (third term). The correlated tunneling term $t_{\rm cor}$ arises from the corresponding processes with the particle not returning to the original site. The functions $f^{(I)}_i(\phi)$ take the explicit form

$$f^I_t(\phi) = T_{II}(\phi) = \cos(\phi/2)^{2I}, \tag{A5}$$

$$\begin{aligned} f^I_{\rm cor}(\phi, \tilde{u}) &= -\sum_{s' \neq I} \frac{T_{I,s'}(\phi) T_{I,s'}(\phi)}{(E_{s'} - E_I + U)/\Omega} \\ &= -\frac{\cos(\phi/2)^{4I}}{4I\tilde{u}} \{F[-2I, 2I\tilde{u}, \\ &\quad 1 + 2I\tilde{u}, \tan(\phi/2)^2] - 1\}, \end{aligned} \tag{A6}$$

$$\begin{aligned} f^I_V(\phi, \tilde{u}) &= \sum_{s' \neq I} \frac{T_{I,s'}(\phi) \bar{T}_{s',I}(\phi)}{(E_{s'} - E_I + U)/\Omega} \\ &= \frac{\cos(\phi/2)^{4I}}{4I\tilde{u}} \{F[-2I, 2I\tilde{u}, 1 + 2I\tilde{u}, \\ &\quad -\tan(\phi/2)^2] - 1\}, \end{aligned} \tag{A7}$$

where $\tilde{u} = U/(4I\Omega)$, and $F(a,b,c,z) = {}_2F_1(a,b,c,z)$ is the hypergeometric function.

[1] I. Bloch, J. Dalibard, and W. Zwerger, Many-body physics with ultracold gases, Rev. Mod. Phys. **80**, 885 (2008).

[2] W. Ketterle and M. Zwierlein, Making, probing and understanding ultracold fermi gases, in *Ultracold Fermi Gases, Proceedings of the International School of Physics "Enrico Fermi"*, edited by M. Inguscio, W. Ketterle, and C. Salomon, Course CLXIV (IOS Press, Amsterdam, 2008); reprinted in Riv. Nuovo Cimento **31**, 247 (2008).

[3] O. Boada, A. Celi, J. I. Latorre, and M. Lewenstein, Quantum Simulation of an Extra Dimension, Phys. Rev. Lett. **108**, 133001 (2012).

[4] A. Celi, P. Massignan, J. Ruseckas, N. Goldman, I. B. Spielman, G. Juzeliunas, and M. Lewenstein, Synthetic Gauge Fields in Synthetic Dimensions, Phys. Rev. Lett. **112**, 043001 (2014).

[5] G. Pagano, M. Mancini, G. Cappellini, P. Lombardi, F. Schäfer, H. Hu, X.-ji Liu, J. Catani, C. Sias, M. Inguscio, and L. Fallani, A one-dimensional liquid of fermions with tunable spin, Nat. Phys. **10**, 198 (2014).

[6] J. S. Krauser, J. Heinze, N. Fläschner, S. Götze, O. Jürgensen, D.-s. Lühmann, C. Becker, and K. Sengstock, Coherent multi-flavour spin dynamics in a fermionic quantum gas, Nat. Phys. **8**, 813 (2012).

[7] J. S. Krauser, U. Ebling, N. Flaschner, J. Heinze, K. Sengstock, M. Lewenstein, A. Eckardt, and C. Becker, Giant spin oscillations in an ultracold fermi sea, Science **343**, 157 (2014).

[8] J. Dalibard, F. Gerbier, G. Juzeliunas, and P. Öhberg, Colloquium: Artificial gauge potentials for neutral atoms, Rev. Mod. Phys. **83**, 1523 (2011).

[9] N. Goldman, G. Juzeliunas, P. Öhberg, and I. B. Spielman, Light-induced gauge fields for ultracold atoms, Rep. Prog. Phys. **77**, 126401 (2014).

[10] B. K. Stuhl, H.-I. Lu, L. M. Aycock, D. Genkina, and I. B. Spielman, Visualizing edge states with an atomic Bose gas in the quantum hall regime, Science **349**, 1514 (2015).

[11] M. Mancini, G. Pagano, G. Cappellini, L. Livi, M. Rider, J. Catani, C. Sias, P. Zoller, M. Inguscio, M. Dalmonte, and L. Fallani, Observation of chiral edge states with neutral fermions in synthetic hall ribbons, Science **349**, 1510 (2015).

[12] H. M. Price, O. Zilberberg, T. Ozawa, I. Carusotto, and N. Goldman, Four-Dimensional Quantum Hall Effect with Ultracold Atoms, Phys. Rev. Lett. **115**, 195303 (2015).

[13] A. Dhar, M. Maji, T. Mishra, R. V. Pai, S. Mukerjee, and A. Paramekanti, Bose-Hubbard model in a strong effective magnetic field: Emergence of a chiral mott insulator ground state, Phys. Rev. A **85**, 041602 (2012).

[14] A. Dhar, T. Mishra, M. Maji, R. V. Pai, S. Mukerjee, and A. Paramekanti, Chiral mott insulator with staggered loop currents in the fully frustrated Bose-Hubbard model, Phys. Rev. B **87**, 174501 (2013).

[15] A. Tokuno and A. Georges, Ground states of a Bose–Hubbard ladder in an artificial magnetic field: Field-theoretical approach, New J. Phys. **16**, 073005 (2014).

[16] M. Piraud, F. Heidrich-Meisner, I. P. McCulloch, S. Greschner, T. Vekua, and U. Schollwöck, Vortex and meissner phases of strongly interacting bosons on a two-leg ladder, Phys. Rev. B **91**, 140406 (2015).

[17] S. Greschner, M. Piraud, F. Heidrich-Meisner, I. P. McCulloch, U. Schollwöck, and T. Vekua, Spontaneous Increase of Magnetic Flux and Chiral-Current Reversal in Bosonic Ladders: Swimming against the Tide, Phys. Rev. Lett. **115**, 190402 (2015).

[18] F. Kolley, M. Piraud, I. P. McCulloch, U. Schollwöck, and F. Heidrich-Meisner, Strongly interacting bosons on a three-leg ladder in the presence of a homogeneous flux, New J. Phys. **17**, 092001 (2015).

[19] G. Roux, E. Orignac, S. R. White, and D. Poilblanc, Diamagnetism of doped two-leg ladders and probing the nature of their commensurate phases, Phys. Rev. B **76**, 195105 (2007).

[20] G. Sun, J. Jaramillo, L. Santos, and T. Vekua, Spin-orbit coupled fermions in ladderlike optical lattices at half filling, Phys. Rev. B **88**, 165101 (2013).

[21] M. Piraud, Z. Cai, I. P. McCulloch, and U Schollwöck, Quantum magnetism of bosons with synthetic gauge fields in one-dimensional optical lattices: A density-matrix renormalization-group study, Phys. Rev. A **89**, 063618 (2014).

[22] M. Lacki, H. Pichler, A. Sterdyniak, A. Lyras, V. E. Lembessis, O. Al-Dossary, J. C. Budich, and P. Zoller, Quantum Hall physics with cold atoms in cylindrical optical lattices, Phys. Rev. A **93**, 013604 (2016).

[23] J. C. Budich, C. Laflamme, F. Tschirsich, S. Montangero, and P. Zoller, Synthetic helical liquids with ultracold atoms in optical lattices, Phys. Rev. B **92**, 245121 (2015).

[24] L. Mazza, M. Aidelsburger, H.-H. Tu, N. Goldman, and M. Burrello, Methods for detecting charge fractionalization and winding numbers in an interacting fermionic ladder, New J. Phys. **17**, 105001 (2015).

[25] E. Cornfeld and E. Sela, Chiral currents in one-dimensional fractional quantum hall states, Phys. Rev. B **92**, 115446 (2015).

[26] T.-S. Zeng, C. Wang, and H. Zhai, Charge Pumping of Interacting Fermion Atoms in the Synthetic Dimension, Phys. Rev. Lett. **115**, 095302 (2015).

[27] S. Barbarino, L. Taddia, D. Rossini, L. Mazza, and R. Fazio, Magnetic crystals and helical liquids in alkaline-earth fermionic gases, Nat. Commun. **6**, 8134 (2015).

[28] S. Barbarino, L. Taddia, D. Rossini, L. Mazza, and R. Fazio, Synthetic gauge fields in synthetic dimensions: Interactions and chiral edge modes, New J. Phys. **18**, 035010 (2016).

[29] S. R. Manmana, K. R. A. Hazzard, G. Chen, A. E. Feiguin, and A. M. Rey, SU($n$) magnetism in chains of ultracold alkaline-earth-metal atoms: Mott transitions and quantum correlations, Phys. Rev. A **84**, 043601 (2011).

[30] A. V. Gorshkov, M. Hermele, V. Gurarie, C. Xu, P. S. Julienne, J. Ye, P. Zoller, E. Demler, M. D. Lukin, and A. M. Rey, Two-orbital SU($n$) magnetism with ultracold alkaline-earth atoms, Nat. Phys. **6**, 289 (2010).

[31] X. Zhang, M. Bishof, S. L. Bromley, C. V. Kraus, M. S. Safronova, P. Zoller, A. M. Rey, and J. Ye, Spectroscopic observation of SU($n$)-symmetric interactions in sr orbital magnetism, Science **345**, 1467 (2014).

[32] M. A. Cazalilla and A. M. Rey, Ultracold fermi gases with emergent SU($n$) symmetry, Rep. Prog. Phys. **77**, 124401 (2014).

[33] M. Girardeau, Relationship between systems of impenetrable bosons and fermions in one dimension, J. Math. Phys. **1**, 516 (1960).

[34] T. Kinoshita, Observation of a one-dimensional Tonks-Girardeau gas, Science **305**, 1125 (2004).

[35] B. Paredes, A. Widera, V. Murg, O. Mandel, S. Fölling, I. Cirac, G. V. Shlyapnikov, T. W. Hänsch, and I. Bloch, Tonks–Girardeau

gas of ultracold atoms in an optical lattice, Nature (London) **429**, 277 (2004).
[36] M. Baranov, Theoretical progress in many-body physics with ultracold dipolar gases, Phys. Rep. **464**, 71 (2008).
[37] M. A. Baranov, M. Dalmonte, G. Pupillo, and P. Zoller, Condensed matter theory of dipolar quantum gases, Chem. Rev. **112**, 5012 (2012).
[38] C. Trefzger, C. Menotti, and M. Lewenstein, Pair-Supersolid Phase in a Bilayer System of Dipolar Lattice Bosons, Phys. Rev. Lett. **103**, 035304 (2009).
[39] A. Safavi-naini, Ş G. Söyler, G. Pupillo, H. R. Sadeghpour, and B. Capogrosso-Sansone, Quantum phases of dipolar bosons in bilayer geometry, New J. Phys. **15**, 013036 (2013).
[40] A. Macia, G. E. Astrakharchik, F. Mazzanti, S. Giorgini, and J. Boronat, Single-particle versus pair superfluidity in a bilayer system of dipolar bosons, Phys. Rev. A **90**, 043623 (2014).
[41] R. Bendjama, B. Kumar, and F. Mila, Absence of Single-Particle Bose-Einstein Condensation at Low Densities for Bosons with Correlated Hopping, Phys. Rev. Lett. **95**, 110406 (2005).
[42] P. Nozières and D. Saint James, Particle vs. pair condensation in attractive Bose liquids, J. Phys. France **43**, 1133 (1982).
[43] K. P. Schmidt, J. Dorier, A. Läuchli, and F. Mila, Single-particle versus pair condensation of hard-core bosons with correlated hopping, Phys. Rev. B **74**, 174508 (2006).
[44] S. Takayoshi, H. Katsura, N. Watanabe, and H. Aoki, Phase diagram and pair tomonaga-luttinger liquid in a Bose-Hubbard model with flat bands, Phys. Rev. A **88**, 063613 (2013).
[45] M. Tovmasyan, E. P. L. van Nieuwenburg, and S. D. Huber, Geometry-induced pair condensation, Phys. Rev. B **88**, 220510 (2013).
[46] U. Schollwöck, The density-matrix renormalization group, Rev. Mod. Phys. **77**, 259 (2005).
[47] A. Ghosh and S. Yarlagadda, Analysis of the $t_2 - V$ model, Phys. Rev. B **90**, 045140 (2014).
[48] R. Z. Bariev, Integrable spin chain with two- and three-particle interactions, J. Phys. A: Math. Gen. **24**, L549 (1991).
[49] R. W. Chhajlany, P. R. Grzybowski, J. Stasińska, M. Lewenstein, and O. Dutta, Hidden String Order in a Hole Superconductor with Extended Correlated Hopping, Phys. Rev. Lett. **116**, 225303 (2016).
[50] B. Bauer, L. D. Carr, H. G. Evertz, A. Feiguin, J. Freire, S. Fuchs, L. Gamper, J. Gukelberger, E. Gull, S. Guertler, A. Hehn, R. Igarashi, S. V. Isakov, D. Koop, P. N. Ma, P. Mates, H. Matsuo, O. Parcollet, G. Pawłowski, J. D. Picon, L. Pollet, E. Santos, V. W. Scarola, U. Schollwöck, C. Silva, B. Surer, S. Todo, S. Trebst, M. Troyer, M. L. Wall, P. Werner, and S. Wessel, The ALPS project release 2.0: Open source software for strongly correlated systems, J. Stat. Mech. (2011) P05001.
[51] M. Dolfi, B. Bauer, S. Keller, A. Kosenkov, T. Ewart, A. Kantian, T. Giamarchi, and M. Troyer, Matrix product state applications for the ALPS project, Comput. Phys. Commun. **185**, 3430 (2014).
[52] J. Eisert, M. Cramer, and M. B. Plenio, *Colloquium* : Area laws for the entanglement entropy, Rev. Mod. Phys. **82**, 277 (2010).
[53] G. Vidal, J. I. Latorre, E. Rico, and A. Kitaev, Entanglement in Quantum Critical Phenomena, Phys. Rev. Lett. **90**, 227902 (2003).
[54] V. E. Korepin, Universality of Entropy Scaling in One Dimensional Gapless Models, Phys. Rev. Lett. **92**, 096402 (2004).
[55] I. Affleck and A. W. W. Ludwig, Universal Noninteger "Ground-State Degeneracy" in Critical Quantum Systems, Phys. Rev. Lett. **67**, 161 (1991).
[56] C. Holzhey, F. Larsen, and F. Wilczek, Geometric and renormalized entropy in conformal field theory, Nucl. Phys. B **424**, 443 (1994).
[57] P. Calabrese and J. Cardy, Entanglement entropy and quantum field theory, J. Stat. Mech (2004) P06002.
[58] T. D. Kühner, S. R. White, and H. Monien, One-dimensional Bose-Hubbard model with nearest-neighbor interaction, Phys. Rev. B **61**, 12474 (2000).
[59] M. S. Luthra, T. Mishra, R. V. Pai, and B. P. Das, Phase diagram of a bosonic ladder with two coupled chains, Phys. Rev. B **78**, 165104 (2008).
[60] R. V. Pai and R. Pandit, Superfluid, mott-insulator, and mass-density-wave phases in the one-dimensional extended Bose-Hubbard model, Phys. Rev. B **71**, 104508 (2005).
[61] M. Rigol and A. Muramatsu, Ground-state properties of hard-core bosons confined on one-dimensional optical lattices, Phys. Rev. A **72**, 013604 (2005).
[62] M. Eckholt and J. J. García-Ripoll, Correlated hopping of bosonic atoms induced by optical lattices, New J. Phys. **11**, 093028 (2009).
[63] S. D. Huber and E. Altman, Bose condensation in flat bands, Phys. Rev. B **82**, 184502 (2010).
[64] T. Keilmann, S. Lanzmich, I. McCulloch, and M. Roncaglia, Statistically induced phase transitions and anyons in 1D optical lattices, Nat. Commun. **2**, 361 (2011).
[65] G. Möller and N. R. Cooper, Correlated Phases of Bosons in the Flat Lowest Band of the Dice Lattice, Phys. Rev. Lett. **108**, 045306 (2012).
[66] M. Di Liberto, C. E. Creffield, G. I. Japaridze, and C. Morais Smith, Quantum simulation of correlated-hopping models with fermions in optical lattices, Phys. Rev. A **89**, 013624 (2014).
[67] S. Kourtis and C. Castelnovo, Two-dimensional topological order of kinetically constrained quantum particles, Phys. Rev. B **91**, 155134 (2015).
[68] T. Mishra, S. Greschner, and L. Santos, Density-induced geometric frustration of ultra-cold bosons in optical lattices, New J. Phys. **18**, 045016 (2016).